Table 2 Endocrine complications in hypothalamic pituitary axis in Kabuki syndrome

References	Age at endocrine evaluation	Sex	Complications in HP axis	Endocrine data in HP axis Serum hormone levels	Stimulation	Provocative tests Peak levels	Other endocrine data or complications	MRI findings in HP
Kuroki et al. [7]	11 months	F	Precocious puberty	PRL, 38.8 ng/ml (NR: 5–10)	LH-RH	LH, 66.7 ng/dL (NR: 4–63) FSH, 1,141.7 ng/ml (NR: 0–150)	E2, 43.0 pg/mL (NR: 2–10) Advanced bone age	N/D[a]
Niikawa et al. [5]	5 years	M	GH deficiency	N/D	N/D			N/D
Handa et al. [8]	1 year	F	GH deficiency	N/D	Arginine	GH, 8.6 ng/ml (NR: >10)	Premature thelarche	N/D
Franceschini et al. [10]	7 years 6 months	F	Precocious puberty	Increase in gonadotropin secretion	N/D		Advanced bone age	N/D
Satoh et al. [12]	2 years 11 months	M	GH deficiency	IGF-1, 0.32 U/ml	Arginine	GH, 0.8 ng/ml		Abnormal[b]
					Glucagon	GH, 2.5 ng/ml		
Tawa et al. [4]	4 years	M	Diabetes insipidus		Water deprivation	Urine osmolarity, <260 mOsm/kg H_2O[e];		Abnormal[c]
			GH deficiency	IGF-1, 0.40 U/ml	Sleep	GH, 3.6 ng/ml		
Devriendt et al. [11]	1 year 6 months–3 years 6 months	F	Hypothalamic GH deficiency	IGF-1, <10 ng/ml (at 3.5 years of age)	Glucagon	GH, 9.8 ng/ml (at 23 months of age)	Premature thelarche	Normal
						GH, 8.1 ng/ml (3.5 years of age)		
					GRF	GH, 40 ng/ml (18 months of age)		
Gabrielli et al. [9]	9 years	M	GH deficiency	IGF-1, 1.0 U/ml (NR: 0.87–2.06)	Clonidine	GH, 5.2 ng/ml		N/D
					Arginine	GH, 5.0 ng/mL		
					Sleep	GH, 2.7 ng/ml (NR: >3.2)		
Ma et al. [6]	6 years	M	ACTH deficiency		CRH	Cortisol, <6 nmol/L		Normal
						ACTH, 18 pg/ml (NR: 9–52)		
The present case	6 years	F	Diabetes insipidus		Water deprivation	Fig. 1[e]		Abnormal[d]

ACTH adrenocorticotropin hormone, *CT* computed tomography, *E2* estradiol, *FSH* follicle-stimulating hormone, *F* female, *GH* growth hormone, *HP* hypothalamic pituitary, *IGF-I* insulin-like growth factor-I, *LH* luteinizing hormone, *LH-RH* luteinizing hormone releasing hormone, *M* male, *MRI* magnetic resonance imaging, *N/D* not described, *NR* normal range, *PRL* prolactin

[a] CT scans showed normal

[b] Transection of pituitary stalk, atrophic anterior pituitary lobe, ectopic posterior pituitary lobe

[c] Small anterior pituitary lobe, narrow pituitary stalk, absence of high intensity signal of posterior pituitary lobe

[d] Absence of high intensity signal of posterior pituitary lobe

[e] Increase of urine osmolarity with response to vasopressin administration

Discussion

Kabuki syndrome (or Niikawa-Kuroki syndrome; MIM# 147920) was originally described by Niikawa et al. [1] and Kuroki et al. [2] independently in 1981. Both papers reported patients with multiple anomalies and mental retardation syndrome characterized by distinctive facial features. This syndrome was accompanied by various organ anomalies and health-related issues, in particular, structural CNS abnormalities, such as microcephaly, hydrocephalus, Alnord Chiari I malformation and Dandy–Walker malformation are frequently observed in these patients [3]. In contrast, endocrine problems did not seem common in Kabuki syndrome. Premature thelarche, which usually requires no special treatment, was at relatively high frequency (about 20 %) according to the previous review article [5]. Congenital hypothyroidism was found in 3 of 18 children with Kabuki syndrome [13]. In contrast, congenital abnormalities in hypothalamic pituitary axis have rarely been reported. As shown in Table 2, GH deficiency was at the highest complication in the hypothalamic pituitary axis, and most of them were successfully treated with recombinant GH. The second frequent complication was precocious puberty. Pathogenesis of premature thelarche and precocious puberty are, at least in part, overlapped and derived from hypothalamic dysfunction [14]. Two cases showed central DI either with or without a structural abnormality in the pituitary gland. Central DI can be caused by congenital malformation or secondary destruction or degeneration of neurons originating from the supraoptic and paraventricular nuclei of the hypothalamus. The causes of secondary destruction or degeneration include neoplasms, such as a germinoma or craniopharyngioma, Langerhans cell histiocytosis, autoimmune or infectious inflammation, vascular diseases, or trauma [15]. Congenital mid-brain malformation also causes congenital central DI, whereas about half of the cases are classified as the idiopathic type. The present case developed polydipsia and polyuria at 6 years of age, but neither potentially responsible destructive disease nor hypothalamic pituitary dysgenesis was identified, hence the etiology of her central DI would be classified as the idiopathic type. The other case was suggested that central DI might be derived from pituitary dysgenesis, because structural abnormality was observed in MRI. We speculate that the posterior pituitary gland of both cases may have already been partially defective on a congenital basis, and became insufficient to secrete an appropriate level of AVP during the patient's growth and development. Alternatively, it is possible that self destruction or apoptosis of the cells occurred in the posterior lobe of the pituitary gland and finally led to the development of the central DI.

Kabuki syndrome has an estimated incidence of 1 in 32,000 births on the basis of data from "Monitoring for Congenital Anomalies" in Kanagawa Prefecture in Japan [5]. Most of the cases are sporadic, and a few cases were shown to be transmitted from mildly affected parents [16, 17]. Mutations in the *mixed lineage leukemia 2* (*MLL2*) gene were found in 62–75 % of patients with Kabuki syndrome [18–21], thus suggesting that there is a wide range of variable expressivity or the existence of other causal gene(s). Although congenital abnormalities in the pituitary gland or hypothalamus are rare in Kabuki syndrome, the potential for such abnormalities should be taken into account for all Kabuki patients.

The molecular mechanism(s) responsible for the *MLL2* gene mutations on the development of symptoms in Kabuki syndrome remains unknown, and the genotype-phenotype correlation has not been clearly identified. The *MLL2* gene encodes H3-K4 histone methyltransferase which forms a complex assembly with other proteins and regulates the gene transcription [22]. It is possible that variations in interacting proteins or polymorphisms in the *MLL2* gene itself may be responsible for the phenotypic variability of Kabuki syndrome. A biochemical analysis of the MLL2 complex would be useful to better understand the mechanism responsible for the variable expressivity and incomplete penetrance of Kabuki syndrome.

In summary, various potential manifestations of Kabuki syndrome, especially on the hypothalamic pituitary axis should be carefully evaluated. The accumulation of genetic data and clinical symptoms will provide important information to understand the molecular mechanism(s) by which the *MLL2* gene results in the development or clinical variability of Kabuki syndrome.

Conflict of interest The authors declare that they have no conflict of interest.

References

1. Niikawa N, Matsuura N, Fukushima Y, Ohsawa T, Kajii T (1981) Kabuki make-up syndrome: a syndrome of mental retardation, unusual facies, large and protruding ears, and postnatal growth deficiency. J Pediatr 99(4):565–569
2. Kuroki Y, Suzuki Y, Chyo H, Hata A, Matsui I (1981) A new malformation syndrome of long palpebral fissures, large ears, depressed nasal tip, and skeletal anomalies associated with postnatal dwarfism and mental retardation. J Pediatr 99(4):570–573
3. Ben-Omran T, Teebi AS (2005) Structural central nervous system (CNS) anomalies in Kabuki syndrome. Am J Med Genet A 137(1):100–103
4. Tawa R, Kaino Y, Ito T, Goto Y, Kida K, Matsuda H (1994) A case of Kabuki make-up syndrome with central diabetes insipidus and growth hormone neurosecretory dysfunction. Acta Paediatr Jpn 36(4):412–415
5. Niikawa N, Kuroki Y, Kajii T, Matsuura N, Ishikiriyama S, Tonoki H, Ishikawa N, Yamada Y, Fujita M, Umemoto H et al (1988) Kabuki make-up (Niikawa-Kuroki) syndrome: a study of 62 patients. Am J Med Genet 31(3):565–589

6. Ma KH, Chow SN, Yau FT (2005) Isolated adrenocorticotropin deficiency in a child with Kabuki syndrome. J Pediatr Endocrinol Metab 18(6):607–609
7. Kuroki Y, Katsumata N, Eguchi T, Fukushima Y, Suwa S, Kajii T (1987) Precocious puberty in Kabuki makeup syndrome. J Pediatr 110(5):750–752
8. Handa Y, Maeda K, Toida M, Kitajima T, Ishimaru J, Nagai A, Oka N (1991) Kabuki make-up syndrome (Niikawa-Kuroki syndrome) with cleft lip and palate. J Craniomaxillofac Surg 19(3):99–101
9. Gabrielli O, Bruni S, Bruschi B, Carloni I, Coppa GV (2002) Kabuki syndrome and growth hormone deficiency: description of a case treated by long-term hormone replacement. Clin Dysmorphol 11(1):71–72
10. Franceschini P, Vardeu MP, Guala A, Franceschini D, Testa A, Corrias A, Chiabotto P (1993) Lower lip pits and complete idiopathic precocious puberty in a patient with Kabuki make-up (Niikawa-Kuroki) syndrome. Am J Med Genet 47(3):423–425
11. Devriendt K, Lemli L, Craen M, de Zegher F (1995) Growth hormone deficiency and premature thelarche in a female infant with kabuki makeup syndrome. Horm Res 43(6):303–306
12. Satoh M, Arakawa K, Yokoya S, Morooka K (1993) A case of Kabuki make-up syndrome associated with growth hormone deficiency. Clin Pediatr Endocrinol 2(1):13–16
13. Kawame H, Hannibal MC, Hudgins L, Pagon RA (1999) Phenotypic spectrum and management issues in Kabuki syndrome. J Pediatr 134(4):480–485
14. Argyropoulou MI, Kiortsis DN (2005) MRI of the hypothalamic-pituitary axis in children. Pediatr Radiol 35(11):1045–1055
15. Ghirardello S, Garre ML, Rossi A, Maghnie M (2007) The diagnosis of children with central diabetes insipidus. J Pediatr Endocrinol Metab 20(3):359–375
16. Adam MP, Hudgins L (2005) Kabuki syndrome: a review. Clin Genet 67(3):209–219
17. Matsumoto N, Niikawa N (2003) Kabuki make-up syndrome: a review. Am J Med Genet C Semin Med Genet 117C(1):57–65
18. Ng SB, Bigham AW, Buckingham KJ, Hannibal MC, McMillin MJ, Gildersleeve HI, Beck AE, Tabor HK, Cooper GM, Mefford HC, Lee C, Turner EH, Smith JD, Rieder MJ, Yoshiura K, Matsumoto N, Ohta T, Niikawa N, Nickerson DA, Bamshad MJ, Shendure J (2010) Exome sequencing identifies MLL2 mutations as a cause of Kabuki syndrome. Nat Genet 42(9):790–793
19. Hannibal MC, Buckingham KJ, Ng SB, Ming JE, Beck AE, McMillin MJ, Gildersleeve HI, Bigham AW, Tabor HK, Mefford HC, Cook J, Yoshiura K, Matsumoto T, Matsumoto N, Miyake N, Tonoki H, Naritomi K, Kaname T, Nagai T, Ohashi H, Kurosawa K, Hou JW, Ohta T, Liang D, Sudo A, Morris CA, Banka S, Black GC, Clayton-Smith J, Nickerson DA, Zackai EH, Shaikh TH, Donnai D, Niikawa N, Shendure J, Bamshad MJ (2011) Spectrum of MLL2 (ALR) mutations in 110 cases of Kabuki syndrome. Am J Med Genet A 155A(7):1511–1516
20. Li Y, Bogershausen N, Alanay Y, Simsek Kiper PO, Plume N, Keupp K, Pohl E, Pawlik B, Rachwalski M, Milz E, Thoenes M, Albrecht B, Prott EC, Lehmkuhler M, Demuth S, Utine GE, Boduroglu K, Frankenbusch K, Borck G, Gillessen-Kaesbach G, Yigit G, Wieczorek D, Wollnik B (2011) A mutation screen in patients with Kabuki syndrome. Hum Genet 130(6):715–724
21. Micale L, Augello B, Fusco C, Selicorni A, Loviglio MN, Silengo MC, Reymond A, Gumiero B, Zucchetti F, D'Addetta EV, Belligni E, Calcagni A, Digilio MC, Dallapiccola B, Faravelli F, Forzano F, Accadia M, Bonfante A, Clementi M, Daolio C, Douzgou S, Ferrari P, Fischetto R, Garavelli L, Lapi E, Mattina T, Melis D, Patricelli MG, Priolo M, Prontera P, Renieri A, Mencarelli MA, Scarano G, Monica MD, Toschi B, Turolla L, Vancini A, Zatterale A, Gabrielli O, Zelante L, Merla G (2011) Mutation spectrum of MLL2 in a cohort of kabuki syndrome patients. Orphanet J Rare Dis 6:38
22. Paulussen AD, Stegmann AP, Blok MJ, Tserpelis D, Posma-Velter C, Detisch Y, Smeets EE, Wagemans A, Schrander JJ, van den Boogaard MJ, van der Smagt J, van Haeringen A, Stolte-Dijkstra I, Kerstjens-Frederikse WS, Mancini GM, Wessels MW, Hennekam RC, Vreeburg M, Geraedts J, de Ravel T, Fryns JP, Smeets HJ, Devriendt K, Schrander-Stumpel CT (2011) MLL2 mutation spectrum in 45 patients with Kabuki syndrome. Hum Mutat 32(2):E2018–E2025

BRIEF REPORT

Human Mutation

OFFICIAL JOURNAL

HGVS HUMAN GENOME VARIATION SOCIETY www.hgvs.org

KDM6A Point Mutations Cause Kabuki Syndrome

Noriko Miyake,[1]* Seiji Mizuno,[2] Nobuhiko Okamoto,[3] Hirofumi Ohashi,[4] Masaaki Shiina,[5] Kazuhiro Ogata,[5] Yoshinori Tsurusaki,[1] Mitsuko Nakashima,[1] Hirotomo Saitsu,[1] Norio Niikawa,[6] and Naomichi Matsumoto[1]

[1]Department of Human Genetics, Yokohama City University Graduate School of Medicine, Yokohama, Japan; [2]Department of Pediatrics, Central Hospital, Aichi Human Service Center, Kasugai, Japan; [3]Division of Medical Genetics, Osaka Medical Center and Research Institute for Maternal and Child Health, Izumi, Japan; [4]Division of Medical Genetics, Saitama Children's Medical Center, Iwatsuki, Japan; [5]Department of Biochemistry, Yokohama City University Graduate School of Medicine, Yokohama, Japan; [6]Research Institute of Personalized Health Sciences, Health Science University of Hokkaido, Hokkaido, Japan

Communicated by Garry R. Cutting

Received 7 August 2012; accepted revised manuscript 18 September 2012.
Published online 19 October 2012 in Wiley Online Library (www.wiley.com/humanmutation). DOI: 10.1002/humu.22229

ABSTRACT: Kabuki syndrome (KS) is a rare congenital anomaly syndrome characterized by a unique facial appearance, growth retardation, skeletal abnormalities, and intellectual disability. In 2010, *MLL2* was identified as a causative gene. On the basis of published reports, 55–80% of KS cases can be explained by *MLL2* abnormalities. Recently, de novo deletion of *KDM6A* has been reported in three KS patients, but point mutations of *KDM6A* have never been found. In this study, we investigated *KDM6A* in 32 KS patients without an *MLL2* mutation. We identified two nonsense mutations and one 3-bp deletion of *KDM6A* in three KS cases. This is the first report of *KDM6A* point mutations associated with KS.
Hum Mutat 34:108–110, 2013. © 2012 Wiley Periodicals, Inc.

KEY WORDS: Kabuki syndrome; *KDM6A*; point mutations; chromosome X

Kabuki syndrome (KS; MIM# 147920), first described by Niikawa and Kuroki in 1981, is a rare congenital anomaly syndrome with the characteristic facial features of a long palpebral fissure and eversion of lateral third of the inferior eyelids [Kuroki et al., 1981; Niikawa et al., 1981]. Individuals with KS also show mild to severe intellectual disability, growth retardation, skeletal abnormalities, and a variety of visceral malformations. Although KS is thought to inherit in autosomal dominant fashion, other inheritance patterns have also been considered [Matsumoto and Niikawa, 2003]. In 2010, whole exome sequencing successfully identified loss-of-function mutations in *MLL2* in KS. *MLL2* maps to 12q13.12 and consists of at least 54 coding exons. *MLL2* encodes a histone H3 lysine 4 (H3K4)-specific methyl transferase and plays important roles in the epigenetic control of active chromatin states. On the basis of recent reports of *MLL2* mutations in KS, the mutation detection rate of *MLL2* in KS is 55–80% [Banka et al., 2012]. Among the published mutations, 73.2% (170/232) were truncation type, and pathogenic missense mutations were mainly localized in exon 48 [Banka et al., 2012].

X-linked inheritance has also been implicated in KS. Sex chromosome abnormalities in KS have been reported many times and some of the clinical manifestations are shared with Turner syndrome; patients showing overlapping features, called "Turner–Kabuki" syndrome, have been reported [Bianca et al., 2009; Dennis et al., 1993; Niikawa et al., 1988; Rodriguez et al., 2008; Stankiewicz et al., 2001; Wellesley and Slaney, 1994]. Common structural abnormalities (inversion, translocation, and ring chromosome) involving Xp11 and Yp11 in the pseudoautosomal region were observed in KS, implying the potential involvement of the regions for pathogenesis in KS [Matsumoto and Niikawa, 2003]. In addition, two unrelated KS patients with ring X (p11.2q13) have been reported [McGinniss et al., 1997; Niikawa et al., 1988]. However, an X-linked gene for KS has not been identified until recently. In 2012, complete or partial de novo deletions of *KDM6A* (MIM# 300228) were identified in three patients with KS [Lederer et al., 2012]. *KDM6A* resides at Xp11.3 and encodes the lysine demethylase 6A (KDM6A) demethylating di- and trimethyl-lysine 27 on histone H3 (H3K27) [Lee et al., 2007]. H3K4 methylation by MLL2/3 is linked to the demethylation of H3K27 by KDM6A [Lee et al., 2007]. These authors sequenced *KDM6A* in their series of 22 patients, but found no point mutations [Lederer et al., 2012]. In this study, we investigated *KDM6A* with regard to point mutations in KS after obtaining written informed consents from families of patients. The institutional review board of Yokohama City University School of Medicine approved this study.

To identify *KDM6A* mutations in KS, we examined this gene's 29 coding exons along with its exon–intron boundaries (NM_021140.2) in 32 KS individuals with no *MLL2* mutation, using high-resolution melting analysis combined with direct sequencing. We identified three mutations: c.3717G>A (p.Trp1239*) in patient 1 (male, hemizygous), c.1555C>T (p.Arg519*) in patient 2 (male, hemizygous), and c.3354_3356delTCT (p.Leu1119del) in patient 3 (female, heterozygous) (Fig. 1). Nucleotide numbering reflects cDNA numbering with +1 corresponding to the A of the ATG translation initiation codon in the reference sequence (NM_021140.2), according to journal guidelines (www.hgvs.org/mutnomen). The initiation codon is codon 1. One mutation (c.3354_3356delTCT) occurred de novo; parental samples were unavailable for the other two. Because the two nonsense mutations were outside of the last

Additional Supporting Information may be found in the online version of this article.

*Correspondence to: Noriko Miyake, Department of Human Genetics, Yokohama City University Graduate School of Medicine, 3-9 Fukuura, Kanazawa-ku, Yokohama 236-0004, Japan. E-mail: nmiyake@yokohama-cu.ac.jp or Naomichi Matsumoto, E-mail: naomat@yokohama-cu.ac.jp

Contract grant sponsors: Ministry of Health, Labour, and Welfare (Japan) (to N.Mi., H.S., and N.Ma.); Japan Science and Technology Agency (to N.Ma.); Strategic Research Program for Brain Sciences from the Ministry of Education, Culture, Sports, Science, and Technology of Japan (to N.Ma.); Japan Society for the Promotion of Science (to N.Mi., H.S., and N.Ma.); Strategic Research Promotion of Yokohama City University (to N.Ma.); Takeda Science Foundation (to N.Mi. and N.Ma.).

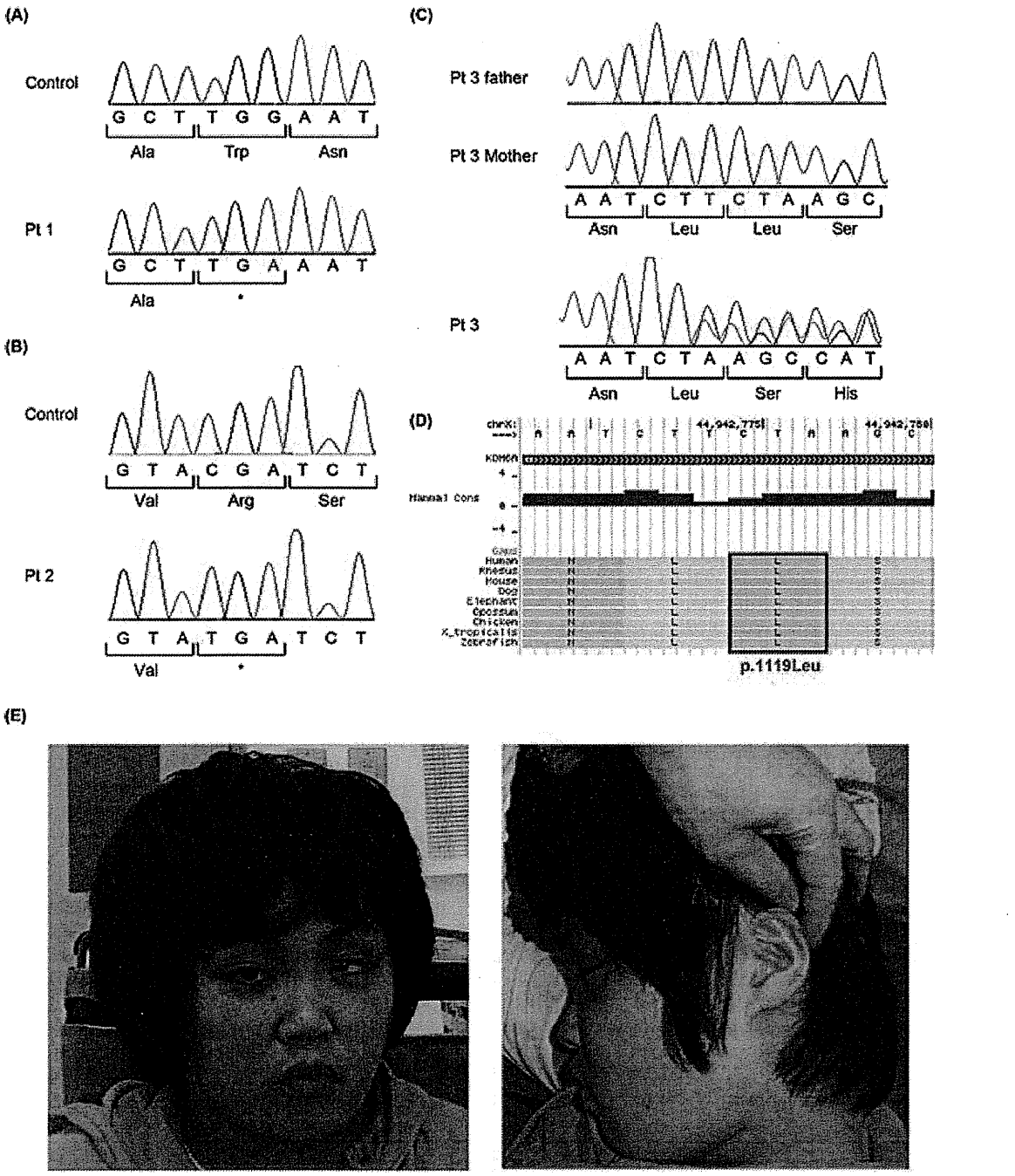

Figure 1. *KDM6A* mutations in three Kabuki syndrome patients. **A–C:** Electropherogram of patient 1: c.3717G>A (p.Trp1239*) (**A**), patient 2: c.1555C>T (p.Arg519*) (**B**), and patient 3: c.3354_3356delTCT (p.Leu1119del) (**C**). Hemizygous changes (**A** and **B**) and a heterozygous change (**C**) can be seen. The altered or deleted nucleotides are written in red. **D:** p. Leu1119 is evolutionarily conserved from zebrafish to human. The position of p.Leu1119 is boxed in red. **E:** Facial photographs of patient 3.

coding exon, and in an exon 55 bp from the 3′ most exon–exon junction, the mutant alleles could be subjected to nonsense-mediated mRNA decay (unfortunately living cells from the patients were unavailable, so we could not test this hypothesis). c.3354_3356delTCT in patient 3 would lead to deletion of one amino acid within the functionally important catalytic Jumonji C (JmjC) domain [Lee et al., 2007]. The amino residue p.Leu1119 is evolutionarily conserved from zebrafish to human (Fig. 1D) and plays an important role in hydrophobic core formation with p.Ile1126 and p.Met1129 to stabilize the JmjC domain [Sengoku and Yokoyama, 2011]. This amino acid deletion may impair helix formation around the mutated residue, resulting in domain destabilization.

Basically, *KDM6A*/*Kdm6a* escapes X-inactivation in humans and mice [Greenfield et al., 1998; Xu et al., 2008]. However, its expression from the inactive X chromosome is lower (15–35%) than that from the active X chromosome in female mice; thus, *Kdm6a* expression

Table 1. Clinical Features of Patients with a *KDM6A* Mutation

	Patient 1	Patient 2	Patient 3
Sex	Male	Male	Female
Mutation	c.3717G>A	c.1555C>T	c.3354_3356delTCT
Protein change	p.Trp1239*	p.Arg519*	p.Leu1119del
De novo status	NA	NA	De novo
Paternal age at birth	34	42	27
Maternal age at birth	33	40	26
Characteristic face	+	+	+
Microcephaly	+	+	–
Long palpebral fissures	+	+	+
Epicanthus	+	–	–
Lower palpebral eversion	+	+	+
Prominent ear	+	+	–
Auricular deformity	+	+	–
Depressed nasal tip	+	+	NA
Short nasal septum	+	+	NA
Abnormal dentition	+	+	–
Hypodontia	+	+	–
High-arched palate	+	+	–
Micrognathia	+	–	–
Short fifth finger	+	–	+
Developmental delay	+ (Severe)	+ (Severe)	+ (Severe)
Intellectual disability	+ (Severe)	+ (Severe)	+ (Severe)
Short stature	+	+	+
Prenatal growth retardation	+ (−1.96 SD)	+	–
Postnatal growth retardation	+	+	+
Cardiovascular abnormality	+	–	–
Joint laxity	+	+	–
Recurrent otitis media	+	–	–
Deafness	+[a]	–	NA
Karyotype	46,XY	46,XY	46,XX

[a]The deafness in patient 1 is conductive because of recurrent otitis media.
KDM6A gene variants were deposited in a gene-specific database (http://www.lovd.Nl/KDM6A).
NA, not analyzed.

in female mice was not twice that in male mice [Xu et al., 2008]. In addition, *UTY* (Yq11.221), a paralog of *KDM6*, has been suspected to partially compensate in males while its function is not well known [Lederer et al., 2012; Xu et al., 2008]. Patient 3 in our study showed a random pattern of X-inactivation with the ratio 57:43 in genomic DNA of peripheral leukocytes. Interestingly, marked skewing of X-inactivation was observed in two female patients reported by Lederer et al. (2012). In their lymphoblast, *KDM6A* deletion was recognized at inactive X chromosome in all 70 mitoses. Here, we propose the threshold model for the pathogenicity of *KDM6A* abnormality (Supp. Fig. S1). The two female patients with a *KDM6A* deletion might not attain the appropriate level of *KDM6A* expression allowing normal development due to existence of specific cells with unfavorable inactivation, whereas male and pure Turner syndrome female with appropriate *KDM6A* expression do not show KS phenotype under assumption of unknown partial functional compensation of *KDM6A* by *UTY* in Y chromosome (only for male) (Supp. Fig. S1).

We reviewed the clinical details of the three patients (Table 1; Supp. Text). All patients were born to unrelated healthy parents. All the three showed severe developmental delay and intellectual disability. Interestingly, patient 3 (female) presented less dysmorphic features and the two male patients 1 and 2 showed a much more severe phenotype with multiple organ involvement (Table 1; Fig. 1E). Null expression of *KDM6A* in males and residual *KDM6A* expression from active X chromosome may explain sex-biased severity (Supp. Fig. S1). Alternatively, it could be explained by a lesser effect of the in-frame mutation in female patient. However, in a previous study, the severity of clinical symptoms varied also among two female patients and a male with a *KDM6A* deletion [Lederer et al., 2012]. More studies of KS patients with *KDM6A* abnormality are necessary. It is likely that the mutation type as well as the X-inactivation pattern in affected organs in females may determine the severity of KS.

In conclusion, we have described the first three point mutations of *KDM6A* in KS. Our three patients out of 32 *MLL2*-negative patients (mutation detection rate: 9.3%) are comparable to the three patients out of 22 *MLL2*-negative patients (13.6%) previously described [Lederer et al., 2012], regardless of the mutation type. The mutation detection rates for *MLL2* (55–80%) plus *KDM6A* (9–13%) in KS suggest that other gene(s) may be found. Because both MLL2 and KDM6A are histone modifiers, the other pathogenic genes might have related functions. Further research is needed to understand the pathomechanisms of KS as well as the role of histone modification in human disease.

Acknowledgments

We thank the patients and their families for participating in this work. We also thank Ms. Y. Yamashita and Ms. S. Sugimoto for technical assistance.

References

Banka S, Veeramachaneni R, Reardon W, Howard E, Bunstone S, Ragge N, Parker MJ, Crow YJ, Kerr B, Kingston H, Metcalfe K, Chandler K, et al. 2012. How genetically heterogeneous is Kabuki syndrome? MLL2 testing in 116 patients, review and analyses of mutation and phenotypic spectrum. Eur J Hum Genet 20:381–388.

Bianca S, Barrano B, Cataliotti A, Indaco L, Ingegnosi C, Ettore G. 2009. Kabuki syndrome and sex chromosomal anomalies: is it really an association? Fertil Steril 91:e6.

Dennis NR, Collins AL, Crolla JA, Cockwell AE, Fisher AM, Jacobs PA. 1993. Three patients with ring (X) chromosomes and a severe phenotype. J Med Genet 30:482–486.

Greenfield A, Carrel L, Pennisi D, Philippe C, Quaderi N, Siggers P, Steiner K, Tam PP, Monaco AP, Willard HF, Koopman P. 1998. The UTX gene escapes X inactivation in mice and humans. Hum Mol Genet 7:737–742.

Kuroki Y, Suzuki Y, Chyo H, Hata A, Matsui I. 1981. A new malformation syndrome of long palpebral fissures, large ears, depressed nasal tip, and skeletal anomalies associated with postnatal dwarfism and mental retardation. J Pediatr 99:570–573.

Lederer D, Grisart B, Digilio MC, Benoit V, Crespin M, Ghariani SC, Maystadt I, Dallapiccola B, Verellen-Dumoulin C. 2012. Deletion of KDM6A, a histone demethylase interacting with MLL2, in three patients with Kabuki syndrome. Am J Hum Genet 90:119–124.

Lee MG, Villa R, Trojer P, Norman J, Yan KP, Reinberg D, Di Croce L, Shiekhattar R. 2007. Demethylation of H3K27 regulates polycomb recruitment and H2A ubiquitination. Science 318:447–450.

Matsumoto N, Niikawa N. 2003. Kabuki make-up syndrome: a review. Am J Med Genet 117C:57–65.

McGinniss MJ, Brown DH, Burke LW, Mascarello JT, Jones MC. 1997. Ring chromosome X in a child with manifestations of Kabuki syndrome. Am J Med Genet 70:37–42.

Niikawa N, Kuroki Y, Kajii T, Matsuura N, Ishikiriyama S, Tonoki H, Ishikawa N, Yamada Y, Fujita M, Umemoto H, Iwama Y, Kondoh I, et al. 1988. Kabuki make-up (Niikawa–Kuroki) syndrome: a study of 62 patients. Am J Med Genet 31:565–589.

Niikawa N, Matsuura N, Fukushima Y, Ohsawa T, Kajii T. 1981. Kabuki make-up syndrome: a syndrome of mental retardation, unusual facies, large and protruding ears, and postnatal growth deficiency. J Pediatr 99:565–569.

Rodriguez L, Diego-Alvarez D, Lorda-Sanchez I, Gallardo FL, Martinez-Fernandez ML, Arroyo-Munoz ME, Martinez-Frias ML. 2008. A small and active ring X chromosome in a female with features of Kabuki syndrome. Am J Med Genet 146A:2816–21.

Sengoku T, Yokoyama S. 2011. Structural basis for histone H3 Lys 27 demethylation by UTX/KDM6A. Genes Dev 25:2266–2277.

Stankiewicz P, Thiele H, Giannakudis I, Schlicker M, Baldermann C, Kruger A, Dorr S, Starke H, Hansmann I. 2001. Kabuki syndrome-like features associated with a small ring chromosome X and XIST gene expression. Am J Med Genet 102:286–292.

Wellesley DG, Slaney S. 1994. Kabuki make-up and Turner syndromes in the same patient. Clin Dysmorphol 3:297–300.

Xu J, Deng X, Watkins R, Disteche CM. 2008. Sex-specific differences in expression of histone demethylases Utx and Uty in mouse brain and neurons. J Neurosci 28:4521–4527.

ORIGINAL ARTICLE

Phenotypic Spectrum of *COL4A1* Mutations: Porencephaly to Schizencephaly

Yuriko Yoneda, MSc,[1] Kazuhiro Haginoya, MD, PhD,[2,3] Mitsuhiro Kato, MD, PhD,[4] Hitoshi Osaka, MD, PhD,[5] Kenji Yokochi, MD, PhD,[6] Hiroshi Arai, MD,[7] Akiyoshi Kakita, MD, PhD,[8] Takamichi Yamamoto, MD, MS, DMSc,[9] Yoshiro Otsuki, MD, PhD,[10] Shin-ichi Shimizu, DDS, PhD,[10] Takahito Wada, MD, PhD,[5] Norihisa Koyama, MD, PhD,[11] Yoichi Mino, MD,[12] Noriko Kondo, MD,[13] Satoru Takahashi, MD, PhD,[14] Shinichi Hirabayashi, MD, PhD,[15] Jun-ichi Takanashi, MD, PhD,[16] Akihisa Okumura, MD, PhD,[17] Toshiyuki Kumagai, MD,[18] Satori Hirai, MD,[7] Makoto Nabetani, MD,[19] Shinji Saitoh, MD, PhD,[20] Ayako Hattori, MD, PhD,[20] Mami Yamasaki, MD, PhD,[21] Akira Kumakura, MD,[22] Yoshinobu Sugo, MD,[1] Kiyomi Nishiyama, PhD,[1] Satoko Miyatake, MD, PhD,[1] Yoshinori Tsurusaki, PhD,[1] Hiroshi Doi, MD, PhD,[1] Noriko Miyake, MD, PhD,[1] Naomichi Matsumoto, MD, PhD,[1] and Hirotomo Saitsu, MD, PhD[1]

Objective: Recently, *COL4A1* mutations have been reported in porencephaly and other cerebral vascular diseases, often associated with ocular, renal, and muscular features. In this study, we aimed to clarify the phenotypic spectrum and incidence of *COL4A1* mutations.

Methods: We screened for *COL4A1* mutations in 61 patients with porencephaly and 10 patients with schizencephaly, which may be similarly caused by disturbed vascular supply leading to cerebral degeneration, but can be distinguished depending on time of insult.

Results: *COL4A1* mutations were identified in 15 patients (21%, 10 mutations in porencephaly and 5 mutations in schizencephaly), who showed a variety of associated findings, including intracranial calcification, focal cortical dysplasia, pontocerebellar atrophy, ocular abnormalities, myopathy, elevated serum creatine kinase levels, and hemolytic anemia. Mutations include 10 missense, a nonsense, a frameshift, and 3 splice site mutations. Five mutations were confirmed as de novo events. One mutation was cosegregated with familial porencephaly, and 2

View this article online at wileyonlinelibrary.com. DOI: 10.1002/ana.23736

Received Jun 8, 2012, and in revised form Aug 6, 2012. Accepted for publication Aug 10, 2012.

Address correspondence to Dr Saitsu, Department of Human Genetics, Yokohama City University Graduate School of Medicine, 3-9 Fukuura, Kanazawa-ku, Yokohama 236-0004, Japan. E-mail: hsaitsu@yokohama-cu.ac.jp

From the [1]Department of Human Genetics, Yokohama City University Graduate School of Medicine, Yokohama; [2]Department of Pediatrics, Tohoku University School of Medicine, Sendai; [3]Department of Pediatric Neurology, Takuto Rehabilitation Center for Children, Sendai; [4]Department of Pediatrics, Yamagata University Faculty of Medicine, Yamagata; [5]Division of Neurology, Clinical Research Institute, Kanagawa Children's Medical Center, Yokohama; [6]Department of Pediatric Neurology, Seirei-Mikatahara General Hospital, Hamamatsu; [7]Department of Pediatric Neurology, Morinomiya Hospital, Osaka; [8]Department of Pathology, Brain Research Institute, University of Niigata, Niigata; [9]Comprehensive Epilepsy Center; [10]Department of Pathology, Seirei Hamamatsu General Hospital, Shizuoka; [11]Department of Pediatrics, Toyohashi Municipal Hospital, Toyohashi; [12]Division of Child Neurology, Tottori University Faculty of Medicine, Yonago; [13]Division of Child Neurology, Department of Brain and Neurosciences, Tottori University Faculty of Medicine, Yonago; [14]Department of Pediatrics, Asahikawa Medical University, Asahikawa; [15]Department of Neurology, Nagano Children's Hospital, Azumino; [16]Department of Pediatrics, Kameda Medical Center, Chiba; [17]Department of Pediatrics, Juntendo University Faculty of Medicine, Tokyo; [18]Aichi Welfare Center for Persons with Developmental Disabilities, Kasugai; [19]Department of Pediatrics, Yodogawa Christian Hospital, Osaka; [20]Department of Pediatrics and Neonatology, Nagoya City University Graduate School of Medical Sciences, Nagoya; [21]Department of Pediatric Neurosurgery, Takatsuki General Hospital, Osaka; and [22]Department of Pediatrics, Kitano Hospital, Tazuke Kofukai Medical Research Institute, Osaka, Japan.

Additional supporting information can be found in the online version of this article.

mutations were inherited from asymptomatic parents. Aberrant splicing was demonstrated by reverse transcriptase polymerase chain reaction analyses in 2 patients with splice site mutations.
Interpretation: Our study first confirmed that *COL4A1* mutations are associated with schizencephaly and hemolytic anemia. Based on the finding that *COL4A1* mutations were frequent in patients with porencephaly and schizencephaly, genetic testing for *COL4A1* should be considered for children with these conditions.
ANN NEUROL 2013;73:48–57

Type IV collagens are basement membrane proteins that are expressed in all tissues, including the vasculature. COL4A1 (α1 chain) and COL4A2 (α2 chain) are the most abundant type IV collagens, and form heterotrimers with a 2:1 stoichiometry (α1α1α2).[1] Mutations in *COL4A1* and *COL4A2* cause sporadic and hereditary porencephaly, a neurological disorder characterized by fluid-filled cysts in the brain that often cause hemiplegia or tetraplegia.[2–4] In addition, a variety of clinical phenotypes, including small vessel disease affecting the brain, eyes, and kidneys, are associated with *COL4A1* abnormality[5,6]: neonatal porencephaly and adult stroke,[7] sporadic extensive bilateral porencephaly resembling hydranencephaly,[8] periventricular leukomalacia with intracranial calcification,[9] HANAC (hereditary angiopathy with nephropathy, aneurysm, and muscle cramps) syndrome,[10,11] Axenfeld–Rieger anomaly with leukoencephalopathy, and adult stroke and intracerebral hemorrhage.[12–14] Notably, *COL4A1* mutations were present in 2 patients with muscle–eye–brain/Walker–Warburg syndrome (MEB/WWS), which is characterized by ocular dysgenesis, neuronal migration defects, and congenital muscular dystrophy, suggesting that *COL4A1* is also involved in normal cortical and muscular development in humans.[15] Consistent with this hypothesis, a mouse model of a heterozygous *COL4A1* mutation (*Col4a1*$^{+/\Delta ex40}$) showed ocular dysgenesis, cortical neuronal localization defects, and myopathy, along with cerebral hemorrhage and porencephaly.[2,15] The phenotypic spectrum of *COL4A1* mutations is expanding; however, the whole spectrum of systemic phenotypes and the incidence of *COL4A1* mutations associated with porencephaly has not been systemically examined.

In this study, we screened for *COL4A1* mutations in 61 patients with porencephaly and 10 patients with schizencephaly, which may be similarly caused by disturbed vascular supply leading to cerebral degeneration, but can be distinguished depending on time of insult.[2–4,16,17] *COL4A1* mutations were identified in 10 patients with porencephaly and 5 patients with schizencephaly, who showed a variety of associated findings, including intracranial calcification, focal cortical dysplasia (FCD), ocular abnormalities, pontocerebellar atrophy, myopathy, elevated serum creatine kinase levels, and hemolytic anemia. Our study demonstrated the importance of genetic testing for *COL4A1* in children with porencephaly or schizencephaly.

Patients and Methods

Patients

A total of 61 patients with porencephaly including a previous cohort with porencephaly,[4] and 10 patients with schizencephaly including a patient who also had porencephaly were analyzed for *COL4A1* mutations. Schizencephaly is defined as transmantle clefts bordered by polymicrogyria in adjacent cortex.[18] The clefts extended through the entire hemisphere, from the ependymal lining of the lateral ventricles to the pial covering of the cortex.[19] The clefts are further divided into those with closed lips and those with open lips. In the clefts with closed lips, the walls affix each other directly, obliterating the cerebrospinal fluid space within the cleft at that point.[20] *COL4A2* mutations were negative for these patients. Genomic DNA was isolated from blood leukocytes according to standard methods, and amplified using an illustra GenomiPhi V2 DNA Amplification Kit (GE Healthcare, Buckinghamshire, UK). The DNA of familial members of patient 6 was isolated from saliva samples using Oragene (DNA Genotek, Kanata, Ontario, Canada). Experimental protocols were approved by the committee for ethical issues at Yokohama City University School of Medicine. All patients were investigated in agreement with the requirements of Japanese regulations.

Mutation Analysis

Exons 1 to 52, covering the entire *COL4A1* coding region, were examined by high-resolution melting (HRM) curve analysis. Samples showing an aberrant melting curve pattern in the HRM analysis were sequenced. Polymerase chain reaction (PCR) primers and conditions are shown in Supplementary Table S1. All novel mutations were verified using original genomic DNA, and screened in 200 Japanese normal controls by HRM analysis. For the family showing de novo mutations, parentage was confirmed by microsatellite analysis, as previously described.[21] Biological parents were confirmed if >4 informative markers were compatible and other markers showed no discrepancy.

Reverse Transcriptase-PCR

Reverse transcriptase (RT)-PCR using total RNA extracted from lymphoblastoid cell lines (LCL) was performed essentially as previously described.[22] Briefly, total RNA was extracted using RNeasy Plus MiniKit (Qiagen, Tokyo, Japan) from LCL with or without 30μM cycloheximide (CHX; Sigma, Tokyo, Japan) incubation for 4 hours. Four micrograms total RNA was subjected to reverse transcription, and 2μl cDNA was used for PCR. Primer sequences are ex20-F (5′-CCCAAAAGGTTTCC CAGGACTACCA-3′) and ex22-R (5′-GTCCGGGCTGACAT TCCACAATTC-3′; for patient 4); and ex22-F (5′-GAATTC-CAGGGCAGCCAGGATTTAT-3′) and ex24-R (5′-CATCTCT GCCAGGCAAACCTCTGT-3′; for patient 7). DNA of each

PCR band was purified by QIAEXII Gel extraction kit (Qiagen; for patient 4) and E.Z.N.A. poly-Gel DNA Extraction kit (Omega Bio-Tek, Norcross, GA; for patient 7), respectively.

Results

Mutation and RT-PCR analysis

COL4A1 abnormalities were identified in 15 patients (Fig 1 and Table). Nine mutations occurred at highly conserved Gly residues in the Gly-X-Y repeat of the collagen triple helical domain. Interestingly, a missense mutation (c.4843G>A [p.Glu1615Lys]) at an evolutionary conserved amino acid and a nonsense mutation (c.4887C>A [p.Tyr1629X]) were found in the carboxy-terminal noncollagenous (NC1) domain. The other 4 mutations include a frameshift mutation (c.2931dupT [p.Gly978TrpfsX15]) and 3 splice site mutations (c.1121-2dupA, c.1382-1G>C, and c.1990+1G>A). None of these mutations was present in 200 Japanese normal controls, and Web-based prediction tools suggested that these mutations are pathogenic (Supplementary Table S2). The c.2842G>A (patient 1), c.3976G>A (patient 2), c.4887C>A (patient 8), c.2689G>A (patient 13), and c.1990+1G>A (patient 14) mutations occurred de novo. The c.3995G>A mutation (patient 3) was not found in the mother's DNA (the father's DNA was unavailable). The c.1121-2dupA (patient 4) and c.2931dupT (patient 6) mutations were found in the asymptomatic fathers. c.1963G>A (patient 10) was found in familial members affected with porencephaly as well as asymptomatic carriers, suggesting incomplete penetrance of the mutation (Supplementary Fig S1). The remaining patients' parental DNA was unavailable.

To examine the mutational effects of the 2 splice acceptor site mutations (c.1121-2dupA and c.1382-1G>C), RT-PCR and sequencing were performed (see Fig 1). c.1121-2dupA caused the deletion of exon 21 from the wild-type *COL4A1* mRNA, resulting in an in-frame 55-amino acid deletion (p.Gly374_Asn429delinsAsp). The effect of c.1382-1G>C was more complicated. There were 3 PCR products amplified from LCL treated with CHX, which inhibits nonsense-mediated mRNA decay (NMD). The middle band corresponded to the wild-type allele. The sequence of the lower mutant band showed a 33bp insertion of intron 22 and an 84bp deletion of all of exon 23 from the use of cryptic splice acceptor and donor sites within intron 22. The change of amino acid sequence from this mutant transcript was a deletion of 29 amino acids and an insertion of 12 amino acids (p.Gly461_Gly489delinsValHisCysGlyAspPheTrpSerHisValThrArg). The upper band was only observed in CHX-treated LCL, but was not evident in the untreated LCL, suggesting that this mutant transcript may undergo NMD. Sequencing of the upper band showed a 61bp insertion of intron 22 from the use of a cryptic splice acceptor site within intron 22, as mentioned above. The product of this mutant transcript leads to a frameshift, creating a premature stop codon (p.Gly461ValfsX31), which is consistent with degradation of the mutant transcript by NMD.

Clinical Features

The clinical information for individuals with *COL4A1* mutations is summarized in the Table, and their representative brain images are shown in Figure 2 and Supplementary Fig S2. *COL4A1* mutations were identified in 10 of 61 patients with porencephaly (16.4%). Of note, *COL4A1* mutations were identified in 5 of 10 patients with schizencephaly (50.0%), revealing a novel association between *COL4A1* mutations and schizencephaly. Thirteen patients were born at term, and 2 patients (patients 1 and 12) were born at preterm. Their body weight was normal at birth except for 5 patients (patients 3, 4, 9, 12, and 15) who were below −2.0 standard deviations. The occipitofrontal circumference was available in 12 patients, and 6 patients (patients 2, 3, 6, 13, 14, and 15) were below −2.0 standard deviations. Two patients (patients 11 and 12) were confirmed to have an antenatal hemorrhage as previously reported.[23,24] Among associated findings with *COL4A1* mutations, a patient showed FCD that was histologically demonstrated (Fig 3A–F). In addition, hemolytic anemia was found in 5 of 15 patients, suggesting that hemolytic anemia may be a novel feature associated with *COL4A1* mutation. Pontocerebellar atrophy along with severe bilateral porencephaly was observed in 2 patients, and a patient showed cerebellar hypoplasia. Previously reported magnetic resonance imaging and systemic findings associated with *COL4A1* mutations were also observed, including intracranial calcification (7 of 15), myopathy (1 of 15; see Fig 3G, H), ocular abnormalities (4 of 15), and elevated serum creatine kinase levels (6 of 15), confirming that these features are useful signs for *COL4A1* testing. Case reports are available in the Supplementary Data.

Discussion

We found a total of 15 novel mutations in this study. Nine mutations occurred at highly conserved Gly residues in the Gly-X-Y repeat of the collagen triple helical domain, suggesting that these mutations may alter the collagen IV $\alpha1\alpha1\alpha2$ heterotrimers.[1,25] We reported for the first time 2 mutations (a nonsense and a missense change) in the NC1 domain. The nonsense mutation

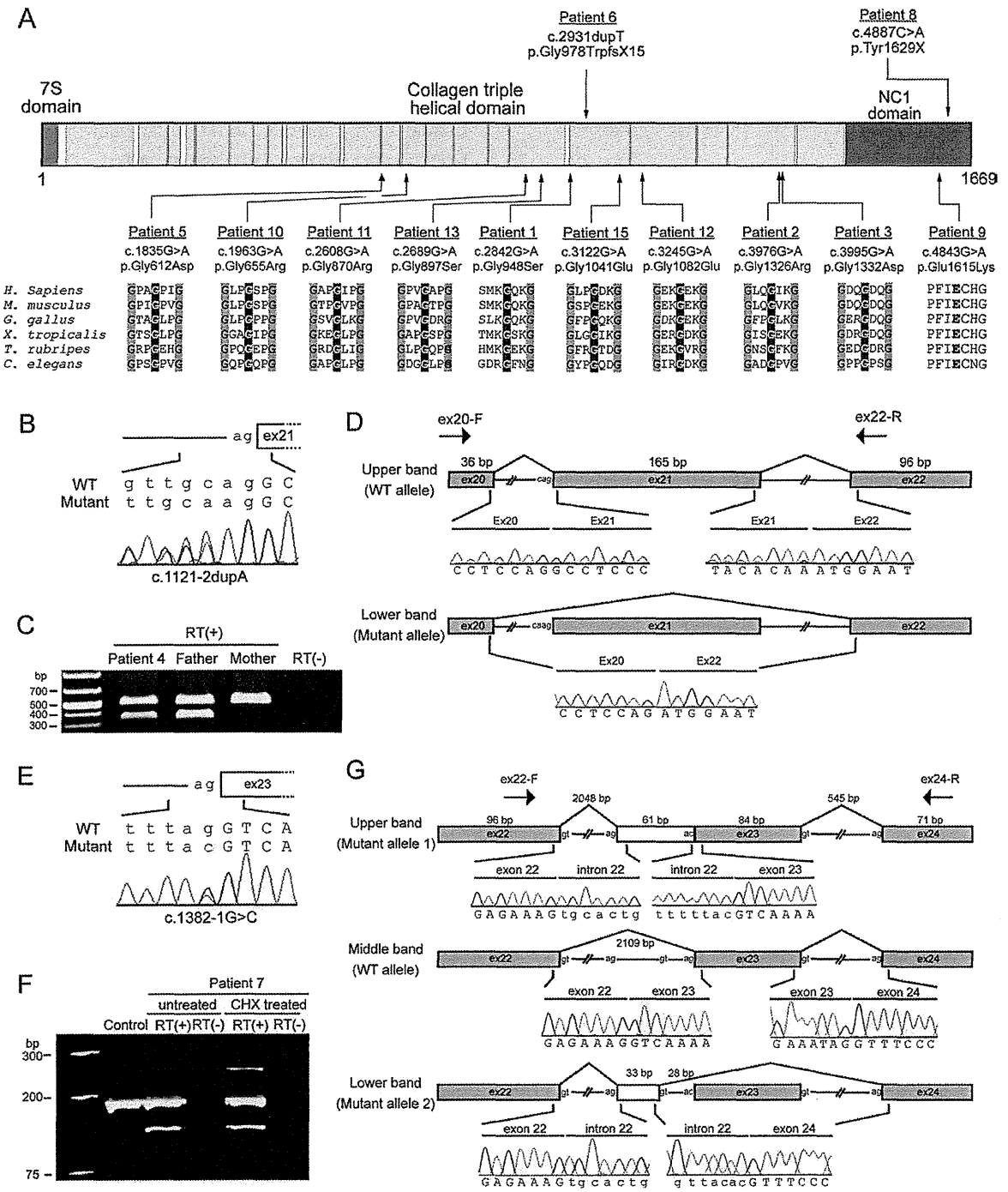

FIGURE 1: *COL4A1* mutations in patients with porencephaly or schizencephaly. (A) Functional domains of COL4A1 protein. The locations of 12 mutations, including 10 missense mutations (bottom), a nonsense mutation, and a frameshift mutation (top) are indicated by arrows. The 7S domain is highlighted with blue and the NC1 domain with red. Gly-X-Y repeats within the collagen triple helical domain are highlighted with yellow. All of the missense mutations occurred at evolutionary conserved amino acids. The positions of the conserved Gly residues in the Gly-X-Y repeats are highlighted in gray. Homologous sequences were aligned using CLUSTALW (http://www.genome.jp/tools/clustalw/). (B) The c.1121-2dupA mutation in intron 20 is colored red. Sequences of exons and introns are presented in upper and lower cases, respectively. (C) Reverse transcriptase (RT)-polymerase chain reaction (PCR) analysis of patient 4 and his parents. (D) Schematic presentation of the wild-type (WT; upper) and mutant (lower) transcripts and primers used for analysis. A single band (500bp), corresponding to the WT allele, was amplified using the mother's cDNA template. Conversely, a lower band was detected from the cDNA from the patient and his father. In the mutant transcript, the 165bp exon 21 was deleted. Sequences of exons and introns are presented in upper and lower cases, respectively. (E) The c.1382-1G>C mutation in intron 22 is colored red. (F) RT-PCR analysis of patient 7 and a control. (G) Schematic representation of the WT and mutant transcripts, and primers used for analysis. A single band (183bp), corresponding to the WT allele, was amplified using a control cDNA template. Conversely, upper and lower bands were detected from the patient's cDNA. The upper band (244bp), which was observed only in cycloheximide (CHX)-treated cells, had a 61bp insertion of intron 22 sequences, leading to a frameshift. Absence of the upper band in untreated lymphoblastoid cell lines strongly suggests that the mutant transcript may undergo nonsense-mediated mRNA decay. The lower band had a 33bp insertion of intron 22 and 84bp deletion of the whole of exon 23, leading to an in-frame 51bp deletion.

TABLE: Clinical features of patients with *COL4A1* mutations

Cases	Age	Sex	Mutation	Inheritance	Brain MRI/ CT findings	CP	Epi	Ocular features	Family history	ID	Hyper-CK	Other
1	14y	M	c.2842G>A (p.Gly948Ser)	de novo	Bilateral POCE, calcification, hemosiderin deposition	Q	+	-	-	+	-	
2	18m	M	c.3976G>A (p.Gly1326Arg)	de novo	Bilateral SCZ, calcification, hemosiderin deposition	Q	+	-	-	+	-	
3	15m	M	c.3995G>A (p.Gly1332Asp)	Absent in mother	Unilateral SCZ, calcification, hemosiderin deposition	H	+	-	-	+	-	
4	6y	M	c.1121-2dupA[1)]	Paternal	Unilateral POCE	H	+	-	-	+	-	FCD
5	2m	F	c.1835G>A (p.Gly612Asp)	ND	Bilateral SCZ, calcification, thin CC, thin brain stem, cerebellar atrophy, absence of SP, hemosiderin deposition, multicystic encephalomalacia,	Q	+	Optic nerve hypoplasia	-	+	+	HA
6	7y	M	c.2931dupT (p.Gly978TrpfsX15)	Paternal	Unilateral POCE	H	+	-	-	+	+	
7	12y	F	c.1382-1G>C[2)]	ND	Unilateral POCE	H	+	-	-	+	+	Myopathy
8	10y	M	c.4887C>A (p.Tyr1629X)	de novo	Unilateral POCE	H	+	-	Hematuria	+	-	
9	3m	F	c.4843G>A (p.Glu1615Lys)	ND	Bilateral POCE, calcification, hypoplastic CC, hemosiderin deposition, thin	Q	+	Microphthalmia Corneal opacity	-	+	-	VSD, HA

TABLE (Continued)

Cases	Age	Sex	Mutation	Inheritance	Brain MRI/ CT findings	CP	Epi	Ocular features	Family history	ID	Hyper-CK	Other
					brain stem, cerebellar atrophy, multicystic encephalomalacia							
10	2y7m	F	c.1963G>A (p.Gly655Arg)	Paternal[3)]	Bilateral POCE	Q	+	-	POCE, Epi	+	-	-
11	1y	F	c.2608G>A (p.Gly870Arg)	ND	Unilateral POCE, calcification	Q	+	Congenital cataract	-	+	-	-
12	1y5m	M	c.3245G>A (p.Gly1082Glu)	ND	Unilateral SCZ with bilateral POCE, calcification, cerebellar hypoplasia	T	+	Congenital cataract	-	+	-	HA, Hematuria
13	3y7m	M	c.2689G>A (p.Gly897Ser)	de novo	Unilateral POCE	Q	+	-	-	+	+	-
14	9m	F	c.1990+1G>A	de novo	Unilateral POCE, hemosiderin deposition	Q	+	-	-	+	+	HA, Hematuria
15	2y	F	c.3122G>A (p.Gly1041Glu)	ND	Unilateral SCZ, hemosiderin deposition	Q	+	-	-	+	+	HA

1) p.Gly374_Asn429delinsAsp change was predicted by mRNA analysis
2) Two alternative protein chages were predicted by mRNA analysis: p.Gly461_Gly489delinsValHisCysGlyAspPheTrpSerHisValThrArg and p.Gly461ValfsX31. y, years; m, months; M, male; F, female; ND, Not determined; POCE, porencephaly, SCZ, schizencephaly; CC, corpus callosum; SP, septum pellucidum; CP, cerebral palsy; H, hemiplegia; T, Triplegia; Q, quadriplegia; Epi, epilepsy; ID, intellectual disability; CK, creatine kinase; FCD, Focal cortical dysplasia; HA, Hemolytic anemia; VSD, ventricular septal defect
3) Co-segregation of the p.Gly655Arg mutation with porencephaly was confirmed.

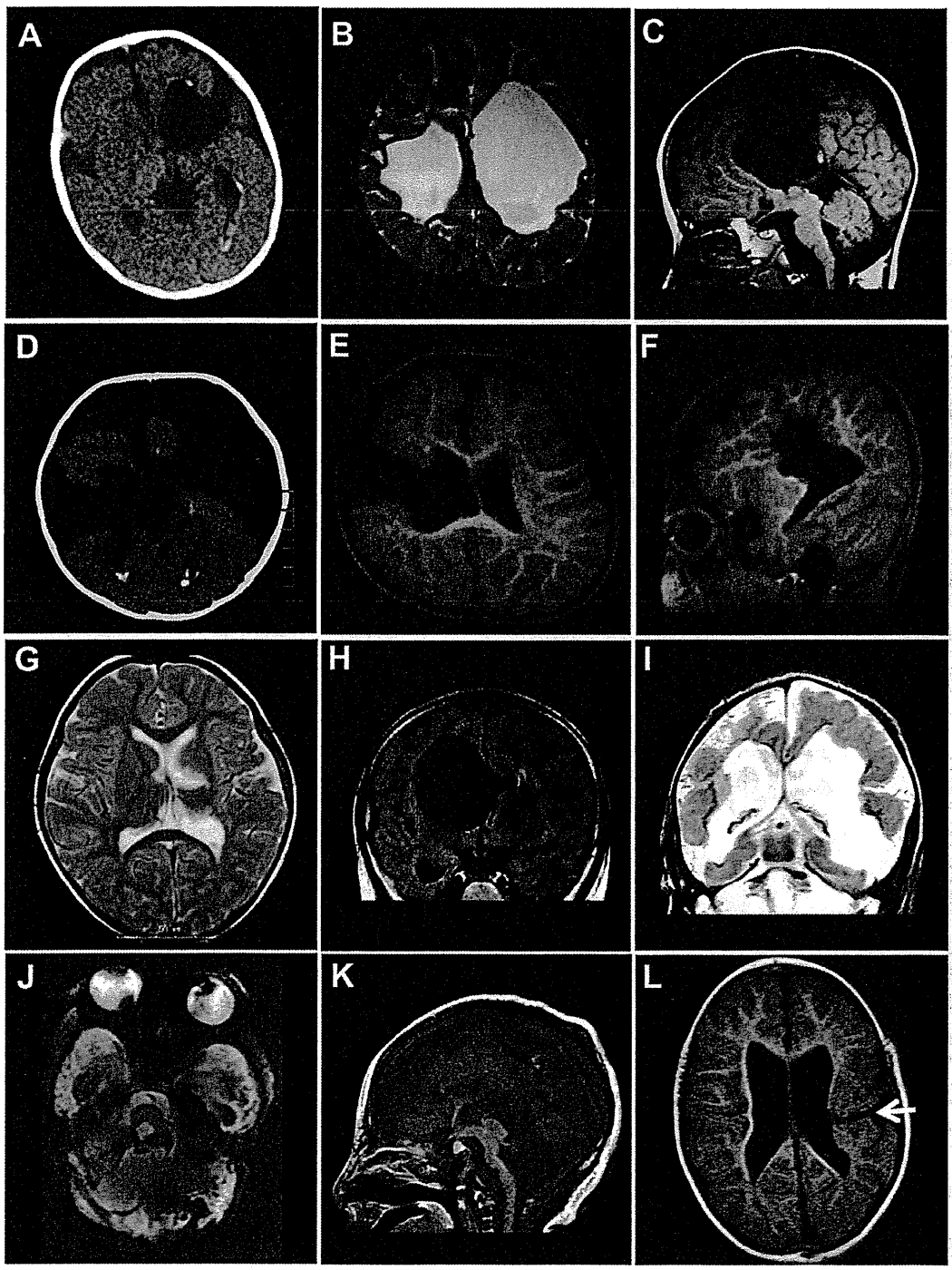

FIGURE 2: Computed tomography (CT) scan (A, D) and magnetic resonance imaging (MRI; B, C, E–L) of patients with *COL4A1* mutations. (A–C) Images of patient 1. (A) The CT scan shows calcification along with the dilated lateral ventricular wall. (B) T2-weighted and (C) T1-weighted images (WIs) at 5 years of age showing bilateral porencephaly. (D) The CT image of patient 2 with schizencephaly shows calcification of the lateral ventricular wall and brain parenchyma. (E, F) T1-WIs of patient 3 show unilateral schizencephaly at 15 months of age. (G) T2-WI of patient 4 at 3 years of age shows parenchymal defect of the left thalamus and basal ganglia due to subependymal hemorrhage. (H) Fluid-attenuated inversion recovery image of patient 7 at 6 years of age showing unilateral porencephaly. (I) T2-WI, (J) T2*-weighted gradient-echo image (WGRE), and (K) T1-WI of patient 9. (I) The MRI at 2 months of age shows bilateral porencephaly with low-intensity lesions along with a deformed ventricular wall, which has hemosiderin deposition and calcification. (J) T2*-WGRE showing hemosiderin deposition in the atrophic cerebellum. The atrophic pontocerebellar structures are also shown in (K). (L) T1-WI of patient 15 showed schizencephaly in the left hemisphere at 2 years of age.

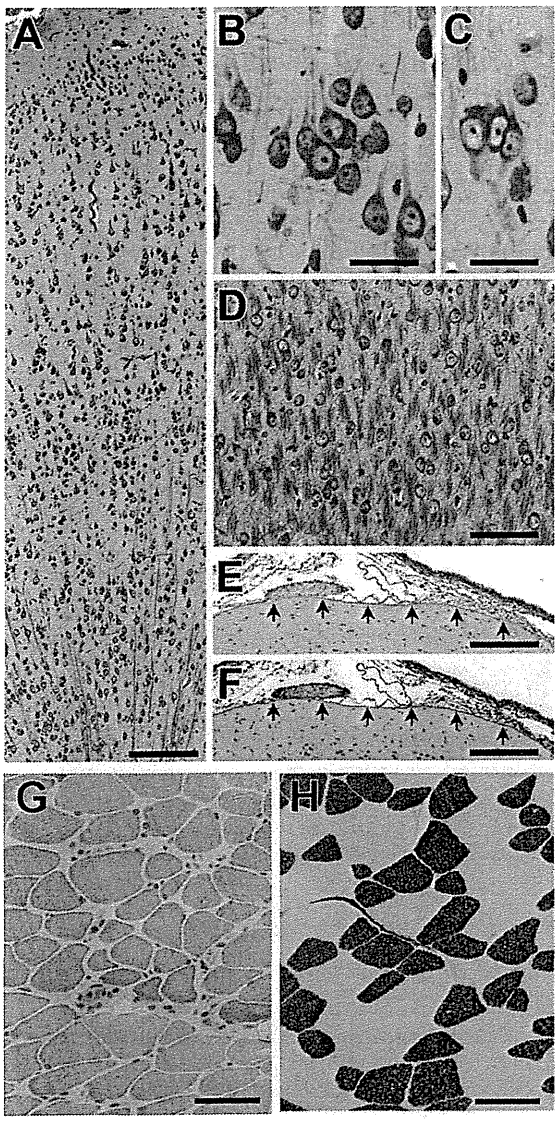

FIGURE 3: Histopathological features of the resected frontal tissue of patient 4 (A–F) and biopsied rectus abdominis muscle of patient 7 (G, H). (A) Low-magnification view of the cortex showing architectural abnormalities. (B, C) Two examples of neuronal clustering. (D) Many neurons scattered within the subcortical white matter. (E, F) Two serial sections demonstrating the superficial layer of the cortex. Note that the basal lamina of the pia mater (arrows in each panel) is continuously labeled with antibodies against collagen type IV (E) and laminin (F). (A–D) Klüver–Barrera stain. (E, F) Immunostained and then counterstained with hematoxylin. (G) Hematoxylin and eosin staining showing variation in fiber size, slightly increased endomysial connective tissue, and internal nuclei. (H) Adenosine triphosphatase (pH 4.5) staining showing type 2B fiber deficiency. There was no increase in number of type 2C fibers. Scale bars indicate 175μm (A, E, F), 30μm (B, C), 80μm (D), and 30μm (G, H).

would cause a truncation of the NC1 domain rather than mRNA degradation by NMD as the mutation was located within 50bp of the exon–intron boundary of the second to last exon (exon 51).[26] The NC1 domains are the sites for molecular recognition through which the stoichiometry of chains in the assembly of triple-helical formation is directed[1]; therefore, these 2 mutations may alter the assembly of the collagen IV α1α1α2 heterotrimers. In addition, the effect of 2 splice site mutations was examined using LCL, suggesting that in-frame deletion/insertion mutant protein should be produced. Thus, it is highly likely that impairment of the collagen IV α1α1α2 heterotrimer assembly caused by mutant α1 chain is a common pathological mechanism of *COL4A1* mutations. The c.2931dupT mutation found in patient 6 and his father might cause severe truncation of COL4A1 protein. It is possible that the truncation of COL4A1 protein can also impair α1α1α2 heterotrimer assembly similar to substitutions of conserved Gly residues in the Gly-X-Y repeat. Alternatively, the mutant transcript might undergo NMD, and haploinsufficiency of *COL4A1* might cause a weakness of basement membrane. Biological analysis using patients' cells will clarify these possibilities.

COL4A1 mutations in schizencephaly were first demonstrated in this study. Schizencephaly was used by Yakovlev and Wadsworth in 1946 to describe true clefts formed in the brain as a result of failure of development of the cortical mantle in the zones of cleavage of the primary cerebral fissures.[19] Schizencephaly is differentiated from clefts in the central mantle that arise as the result of a destruction of the cerebral tissues, which they called encephalocrastic porencephalies, now known simply as porencephaly.[19] Schizencephaly has been understood as a neuronal migration disorder, because the clefts are lined by abnormal gray matter, described as polymicrogyria. Conversely, porencephaly is understood to be a postmigration accident resulting in lesions, without gray matter lining the clefts or an associated malformation of cortical development. It has been suggested that both schizencephaly and porencephaly are caused by encephaloclastic regions, and can be distinguished depending on time of insult.[16,17] The present study clearly demonstrated that *COL4A1* mutations caused both porencephaly and schizencephaly, supporting the same pathological mechanism for these 2 conditions.

The genes responsible for FCD have been elusive, despite extensive investigation. The pathological features of the cortical tubers of tuberous sclerosis (TSC) may be indistinguishable from those of FCD. Apart from FCD due to TSC, there is only 1 gene that may explain the genetic basis of FCD, where a homozygous mutation in *CNTNAP2* has been identified in Amish children with FCD, macrocephaly, and intractable seizures.[27] Surprisingly, the present study discovered a patient with FCD

and porencephaly, in whom aberrant splicing was demonstrated and FCD1A was pathologically confirmed using resected brain tissues. A recent report revealed *COL4A1* mutations in 2 patients with MEB/WWS showing cobblestone lissencephaly,[15] and abnormal cortical development has been observed in mouse models of *COL4A1* mutations.[15,28] Thus, it is possible that *COL4A1* mutations are involved in cerebral cortical malformations, including FCD. Identification of a greater number of cases is required to confirm the association between *COL4A1* mutations and cortical malformations in humans.

In a few children, the sequelae were much more severe than would be expected on the basis of their imaging findings. This is of importance when counseling parents with regard to prediction of neurodevelopmental outcome.

Two patients with *COL4A1* mutations showed intracranial calcification, pontocerebellar atrophy, ocular abnormalities, and hemolytic anemia associated with severe bilateral porencephaly (patient 9) or schizencephaly (patient 5). Severe hemorrhagic destructive lesions in the cerebrum were observed in these patients, and T2* images also showed hemorrhage in the cerebellum, which may have resulted in a thin brainstem and severe cerebellar atrophy. Thus, these 2 patients could be considered as the most severe manifestations affecting the developing brain and eyes. A common feature of the 2 patients is hemolytic anemia of an unknown cause, which required frequent blood transfusions. Five of 15 patients with *COL4A1* mutations showed hemolytic anemia. Interestingly, 2 reports have demonstrated that mouse *Col4a1* mutants showed a significant reduction in red blood cell (RBC) number and hematocrit.[28,29] Given that *Col4a1* mutations lead to hemorrhage, chronic hemorrhage is possibly involved in RBC loss. Alternatively, the *Col4a1* mutation may directly affect blood progenitor cells, as they transmigrate across basement membranes before entering the peripheral blood.[30] Hemolytic anemia in patients with *COL4A1* mutations would imply the latter explanation. Further studies are required to clarify how *COL4A1/Col4a1* mutations are involved in anemia.

In summary, we found 15 mutations in *COL4A1* among 71 patients with porencephaly or schizencephaly, showing an unexpectedly high percentage of mutations (about 21%) in these patients. Fourteen patients with *COL4A1* mutations had no family history of cerebral palsy. The 15 patients with *COL4A1* mutations showed a variety of phenotypes, further expanding the possible clinical spectrum of *COL4A1* mutations to include schizencephaly, FCD, pontocerebellar atrophy, and hemolytic anemia. Genetic testing for *COL4A1* should be recommended for children with porencephaly and schizencephaly.

Acknowledgment

This work was supported by research grants from the Ministry of Health, Labor, and Welfare (K.H., M.K., H.O., N.Mi., N.Ma., H.S.), Japan Science and Technology Agency (N.Ma.), and Strategic Research Program for Brain Sciences (11105137 to N.Ma.), a Grant-in-Aid for Scientific Research on Innovative Areas (Foundation of Synapse and Neurocircuit Pathology) from the Ministry of Education, Culture, Sports, Science, and Technology of Japan (11001956 to N.Ma.), a Grant-in-Aid for Scientific Research from the Japan Society for the Promotion of Science (H.O., N.Ma.), a Grant-in-Aid for Young Scientists from the Japan Society for the Promotion of Science (H.D., N.Mi., H.S.), and a grant from the Takeda Science Foundation (N.Mi., N.Ma.). This work was performed at the Advanced Medical Research Center, Yokohama City University, Japan.

We thank the patients and their family members for their participation in this study.

Authorship

Y.Y. and K.H. contributed equally to this work.

Potential Conflicts of Interest

Nothing to report.

References

1. Khoshnoodi J, Pedchenko V, Hudson BG. Mammalian collagen IV. Microsc Res Tech 2008;71:357–370.
2. Gould DB, Phalan FC, Breedveld GJ, et al. Mutations in Col4a1 cause perinatal cerebral hemorrhage and porencephaly. Science 2005;308:1167–1171.
3. Breedveld G, de Coo IF, Lequin MH, et al. Novel mutations in three families confirm a major role of COL4A1 in hereditary porencephaly. J Med Genet 2006;43:490–495.
4. Yoneda Y, Haginoya K, Arai H, et al. De novo and inherited mutations in COL4A2, encoding the type IV collagen alpha2 chain cause porencephaly. Am J Hum Genet 2012;90:86–90.
5. Vahedi K, Alamowitch S. Clinical spectrum of type IV collagen (COL4A1) mutations: a novel genetic multisystem disease. Curr Opin Neurol 2011;24:63–68.
6. Lanfranconi S, Markus HS. COL4A1 mutations as a monogenic cause of cerebral small vessel disease: a systematic review. Stroke 2010;41:e513–e518.
7. van der Knaap MS, Smit LM, Barkhof F, et al. Neonatal porencephaly and adult stroke related to mutations in collagen IV A1. Ann Neurol 2006;59:504–511.
8. Meuwissen ME, de Vries LS, Verbeek HA, et al. Sporadic COL4A1 mutations with extensive prenatal porencephaly resembling hydranencephaly. Neurology 2011;76:844–846.

9. Livingston J, Doherty D, Orcesi S, et al. COL4A1 Mutations associated with a characteristic pattern of intracranial calcification. Neuropediatrics 2011;42:227–233.
10. Plaisier E, Gribouval O, Alamowitch S, et al. COL4A1 mutations and hereditary angiopathy, nephropathy, aneurysms, and muscle cramps. N Engl J Med 2007;357:2687–2695.
11. Alamowitch S, Plaisier E, Favrole P, et al. Cerebrovascular disease related to COL4A1 mutations in HANAC syndrome. Neurology 2009;73:1873–1882.
12. Coutts SB, Matysiak-Scholze U, Kohlhase J, Innes AM. Intracerebral hemorrhage in a young man. CMAJ 2011;183:E61–E64.
13. Sibon I, Coupry I, Menegon P, et al. COL4A1 mutation in Axenfeld-Rieger anomaly with leukoencephalopathy and stroke. Ann Neurol 2007;62:177–184.
14. Weng YC, Sonni A, Labelle-Dumais C, et al. COL4A1 mutations in patients with sporadic late-onset intracerebral hemorrhage. Ann Neurol 2012;71:470–477.
15. Labelle-Dumais C, Dilworth DJ, Harrington EP, et al. COL4A1 mutations cause ocular dysgenesis, neuronal localization defects, and myopathy in mice and Walker-Warburg syndrome in humans. PLoS Genet 2011;7:e1002062.
16. Friede R. Porencephaly, hydranencephaly, multicystic encephalopathy. In: Developmental neuropathology. 2nd ed. Berlin, Germany: Springer-Verlag, 1989:28–43.
17. Govaert P. Prenatal stroke. Semin Fetal Neonatal Med 2009;14: 250–266.
18. Barkovich AJ, Guerrini R, Kuzniecky RI, et al. A developmental and genetic classification for malformations of cortical development: update 2012. Brain 2012;135:1348–1369.
19. Yakovlev PI, Wadsworth RC. Schizencephalies; a study of the congenital clefts in the cerebral mantle; clefts with fused lips. J Neuropathol Exp Neurol 1946;5:116–130.
20. Barkovich AJ, Kjos BO. Schizencephaly: correlation of clinical findings with MR characteristics. AJNR Am J Neuroradiol 1992;13: 85–94.
21. Saitsu H, Kato M, Mizuguchi T, et al. De novo mutations in the gene encoding STXBP1 (MUNC18–1) cause early infantile epileptic encephalopathy. Nat Genet 2008;40:782–788.
22. Saitsu H, Kato M, Okada I, et al. STXBP1 mutations in early infantile epileptic encephalopathy with suppression-burst pattern. Epilepsia 2010;51:2397–2405.
23. Lichtenbelt KD, Pistorius LR, De Tollenaer SM, et al. Prenatal genetic confirmation of a COL4A1 mutation presenting with sonographic fetal intracranial hemorrhage. Ultrasound Obstet Gynecol 2012;39:726–727.
24. de Vries LS, Koopman C, Groenendaal F, et al. COL4A1 mutation in two preterm siblings with antenatal onset of parenchymal hemorrhage. Ann Neurol 2009;65:12–18.
25. Engel J, Prockop DJ. The zipper-like folding of collagen triple helices and the effects of mutations that disrupt the zipper. Annu Rev Biophys Biophys Chem 1991;20:137–152.
26. Nagy E, Maquat LE. A rule for termination-codon position within intron-containing genes: when nonsense affects RNA abundance. Trends Biochem Sci 1998;23:198–199.
27. Strauss KA, Puffenberger EG, Huentelman MJ, et al. Recessive symptomatic focal epilepsy and mutant contactin-associated protein-like 2. N Engl J Med 2006;354:1370–1377.
28. Favor J, Gloeckner CJ, Janik D, et al. Type IV procollagen missense mutations associated with defects of the eye, vascular stability, the brain, kidney function and embryonic or postnatal viability in the mouse, Mus musculus: an extension of the Col4a1 allelic series and the identification of the first two Col4a2 mutant alleles. Genetics 2007;175:725–736.
29. Van Agtmael T, Bailey MA, Schlotzer-Schrehardt U, et al. Col4a1 mutation in mice causes defects in vascular function and low blood pressure associated with reduced red blood cell volume. Hum Mol Genet 2010;19:1119–1128.
30. Janowska-Wieczorek A, Marquez LA, Nabholtz JM, et al. Growth factors and cytokines upregulate gelatinase expression in bone marrow CD34(+) cells and their transmigration through reconstituted basement membrane. Blood 1999;93:3379–3390

CLINICAL REPORT

AMERICAN JOURNAL OF medical genetics PART A

A Case of Cerebral Hypomyelination With Spondylo-epi-Metaphyseal Dysplasia

Shihoko Kimura-Ohba,[1]* Kuriko Kagitani-Shimono,[1,2] Natsuko Hashimoto,[1] Shin Nabatame,[1] Takeshi Okinaga,[1] Akira Murakami,[3] Noriko Miyake,[3] Naomichi Matsumoto,[3] Hitoshi Osaka,[4] Keiko Hojo,[5] Reiko Tomita,[5] Masako Taniike,[2] and Keiichi Ozono[1]

[1]Department of Pediatrics, Osaka University Graduate School of Medicine, Osaka, Japan

[2]Department of Child Development, United Graduate School of Child Development, Osaka University Graduate School of Medicine, Osaka, Japan

[3]Department of Human Genetics, Yokohama City University Graduate School of Medicine, Kanagawa, Japan

[4]Division of Pediatric Neurology, Kanagawa Children's Medical Center, Kanagawa, Japan

[5]Todaiji Medical-Educational Center, Nara, Japan

Manuscript Received: 14 August 2011; Manuscript Accepted: 7 September 2012

We reported on a male patient with rare leukoencephalopathy and skeletal abnormalities. The condition was first noticed as a developmental delay, nystagmus and ataxia at 1 year of age. At 4 years of age, he was diagnosed as hypomyelination with skeletal abnormalities from clinical features, brain magnetic resonance imaging (MRI) and skeletal X-rays. His brain MRI revealed diffuse hypomyelination. These findings suggested the classical type of Pelizaeus–Merzbacher disease (PMD) caused by proteolipid protein *(PLP)-1* gene or Pelizaeus–Merzbacher-like disease (PMLD). However, we found neither mutation nor duplication of *PLP-1*. The patient had severe growth retardation and general skeletal dysplasia compatible with spondylo-epi-metaphyseal dysplasia; however the mutation of discoidin domain receptor *(DDR) 2* gene was absent. The co-morbidity of hypomyelination with skeletal abnormalities is rare. We performed array CGH and no causal copy number variation was recognized. Alternatively, this condition may have been caused by a mutation of the gene encoding a molecule that functions in both cerebral myelination and skeletal development. © 2012 Wiley Periodicals, Inc.

Key words: Pelizaeus–Merzbacher disease; cerebral hypomyelination; spondylo-epi-metaphyseal dysplasia

How to Cite this Article:
Kimura-Ohba S, Kagitani-Shimono K, Hashimoto N, Nabatame S, Okinaga T, Murakami A, Miyake N, Matsumoto N, Osaka H, Hojo K, Tomita R, Taniike M, Ozono K. 2013. A case of cerebral hypomyelination with spondylo-epi-metaphyseal dysplasia.
Am J Med Genet Part A 161A:203–207.

INTRODUCTION

Classical/connatal Pelizaeus–Merzbacher disease (PMD; #OMIM 312080) is one of the dysmyelinating/hypomyelinating disorders which are characterize by a primary loss of myelin with a relative sparing of axons; and they appears to relate to inadequate myelinogenesis rather than myelin breakdown [Powers, 2004]. PMD is caused by missense mutations, duplication or deletions in the proteolipid protein *(PLP)-1* gene on chromosome Xq22 [Inoue et al., 1999; Lazzarini et al., 2004]. Hence, the lesions are restricted to the CNS in these diseases.

Common symptoms of connatal and classical types of PMD are nystagmus, extrapyramidal symptoms, and psychomotor deterioration. The onset of the classical-type PMD is at several months to several years after birth, whereas these symptoms in connatal type are shown early after birth and progresses rapidly [Lazzarini et al., 2004]. In the classical type, myelination occurs only in the internal capsule, optic radiation or brain stem [Inoue et al., 1999; Kagitani et al., 1999; Lazzarini et al., 2004].

The clinical features of hypomyelinating disorders are variable; however, there has been only one report of its being associated with skeletal abnormality [Neubauer et al., 2006].

In this report, we describe a boy with hypomyelination and spondylo-epi-metaphyseal dysplasia, and also analyzed the candidate genes; discoidin domain receptor *(DDR) 2* and *PLP1* gene.

Additional supporting information may be found in the online version of this article.

*Correspondence to:
Shihoko Kimura-Ohba, Department of Pediatrics, Osaka University Graduate School of Medicine, 2-2 Yamadaoka, Suita, Osaka 565-0871, Japan. E-mail: skimura@ped.med.osaka-u.ac.jp

Article first published online in Wiley Online Library (wileyonlinelibrary.com): 13 December 2012
DOI 10.1002/ajmg.a.35686

Furthermore, copy number polymorphism was screened by comparative genomic hybridization (CGH). To our knowledge, this is a novel case with central hypomyelination and skeletal dysplasia.

CLINICAL REPORT

Patient Report

The patient is an 11-year-old boy and the only child of healthy and nonconsanguineous parents. He was delivered at 40 weeks without asphyxia. Family history was negative for genetic diseases including neurological/neuromuscular diseases, metabolic diseases, and skeletal diseases. His birth weight was 3,088 g. He seemed to have no dysmorphic features and no neurological symptoms at birth. He gained head control at 4 months, sat alone at 8 months, stood while holding a support at 10 months and could walk in a walker at 1 year of age. However, he could never stand up without support because of contractures of his knees and ankles. He began to speak words at around 12 months. The motor deterioration was recognized subsequently and he could only sit alone at the age of 2. Mild growth retardation was manifested, with a weight of 9,060 g (−1.2 SD), height of 76 cm (−1.8 SD) and head circumference of 46 cm (−1.2 SD) at the age of 18 months.

At the age of 4, he first visited our hospital. Magnetic resonance imaging (MRI) of the brain revealed hypomyelination except the posterior limbs of the internal capsule. X-ray analysis of limbs and vertebrae revealed the following abnormal findings: delayed appearance of epiphyses, short, flared, and broad metaphyses and flattened vertebrae (Fig. 2a–c), which were already indicated at 2 years of age. Nystagmus was first noticed at 4 years of age. He had had continuous wheezing until the age of 5. Vomiting appeared when the patient was around 7 years old and got worse at 10 years of age. He was diagnosed as gastroesophageal reflex and hiatus hernia, for which Nissen fundoplication was performed. Bronchography revealed tracheomalacia and membranous stenosis.

At the age of 11, his height was 107 cm (−5.5 SD); and weight, 21.3 kg (−2.1 SD). The short stature had become obvious since the age of 5 or 6 years. He had a depressed nasal bridge, mildly hypoplastic midface and anteverted nose, a long smooth philtrum and a high palate. There was no sign of hypertelorism. He had a narrowed chest with short ribs. Lordoscoliosis was noticed on the spine position. His hands were small and puffy with short fingers. His feet were also puffy with flattened arches, clubbed fingers, and spastic ankles. The joints of limbs were prominent and showed contractures. Whereas the deformities of the upper limbs were mild, the lower ones showed severe contractures; and he could hardly extend or bend his knees and ankles by himself over 60°. Slow rotatory and lateral nystagmus was noticed, and he could not gaze. The left eye had external strabismus (exotropia). Deep tendon reflexes were absent in the lower extremities because of their articular contracture. Babinski's reflexes were positive on both legs and there was no sign of muscular hypotonia. The nose–finger–nose test revealed dysdiadochokinesia. Severe truncal ataxia was also present. Although he could understand most of daily conversation, his speech was slurred with a hoarse voice. Neither corneal muddiness nor cherry red spots were present, but funduscopic examination revealed bilateral optic atrophy. His developmental quotient (DQ) by Kyoto Scale of Psychological Development 2001 was 47 at 9 years of age (cognitive-adaptive; 40, language-social 55).

Laboratory results of a routine blood and endocrine functions were normal. Both oligoclonal band and myelin basic protein (MBP) in the cerebrospinal fluid (CSF) were absent. Lysosomal enzyme activities, including β-galactosidase, β-hexosaminidase, α-galactosidase, α-fucosidase, and arylsulfatase A, and assay of very-long unsaturated fatty acids were within normal ranges. Screening for urinary mucopolysaccharides was negative. G-banding analysis revealed no chromosomal aberrations.

Electroencephalography showed slow basic-wave activity for his age, low amplitude (<50 μV) and no spikes. The evoked potentials revealed the following: brainstem auditory evoked potential (BAEPs) showed only the 1st and delayed 5th waves (latencies of 5th waves; left 7.02, right 6.28 sec). Visually evoked potentials showed no cortical response. Short sensory-evoked potentials were also absent. In contrast, motor and sensory nerve conductive velocities and F-waves were normal.

The brain MRI and MR spectroscopic (MRS) imaging were shown in Figure 1a–c, which indicated hypomyelination same as the findings at 4 years of age. MRI of the spine showed transformation of the vertebral bodies, irregular vertebral spaces and marked lordoscoliosis (Fig. 2d,e).

The skeletal survey revealed the following bone changes: Vertebral bodies were oval shaped and flattened. C1–C2 instability was absent. In the pelvis, flared iliac wings, short ischia, and convexed upper acetabular margins were observed (Fig. 2h). In the hands, a few of the small carpal bones were smaller than normal and calcified soft tissue was observed around the carpals. The proximal phalanx showed a cone-shaped epiphysis with an irregular metaphysis. Furthermore, the metacarpals were shorter than normal. There was deformity of the caput ulnae (Fig. 2g). In the foot, the toes were short and broad. There was poor ossification of the knee joints (Fig. 2i). In the lower limbs metaphyseal dysplasia was less severe than that in the upper ones. Stippled calcification was present on the lateral bodies of the sacral bones, the femoral heads, and on and around the epiphyses of tubular bones. In addition, the bone-mineral content of all the tubular bones was decreased. These skeletal findings were compatible with the diagnosis of spondylo-epi-metaphyseal dysplasia of the short limb-hand type (OMIM#271665).

At 14 years of age, respiratory failure appeared at episode of infection and tracheostomy was performed ultimately after the second episode of respiratory failure at the age of 16.

Genetic Analysis

Experimental protocols were approved by Institutional Review board (IRB) of Osaka University Hospital and performed after informed consent. DNA was extracted from whole blood using Quick Gene DNA whole blood kit S (QuickGene-800 FUJIFILM, Tokyo, Japan). The Discoidin domain receptor 2 gene (*DDR2*) responsible for spondylo-epi-metaphyseal dysplasia with short limb-hand type [al-Gazali et al., 1996; Cormier-Daire, 2008; Bargal et al., 2009] and the *PLP1* gene were analyzed by polymerase chain reaction (PCR) sequencing (*DDR2* primer data was shown in the Supplemental Data [eTable S1 available in Supporting Information

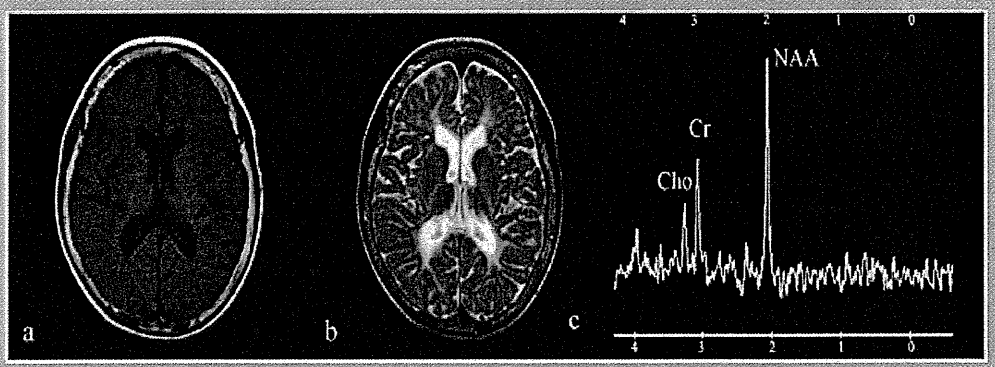

FIG. 1. T1 (a) and T2 (b)-weighted cerebral MRI are shown. In the T1-weighted image, the white matter shows isointensity, same as the gray matter; whereas the internal capsule shows high signal intensity. In the T2-weighed image, the white matter, including the internal capsule, shows diffuse high-signal intensity. c: MR spectra in the right-periventricular white matter. The *N*-acetyl-aspartate [NAA] level shows no decrease; and the choline level shows no increase.

online] and primer and PCR information of *PLP1* are available on request.) [Osaka et al., 1999]. *DDR2* and *PLP1* revealed no sequence abnormalities.

Microarray analysis of the patient was performed using cytogenetics Whole-Genome 2.7M array (Affymetrix, Santa Clara, CA) and Agilent SurePrint G3 human CGH array 2 × 400 K (Agilent, Invitrogen, Santa Clara, CA) [Miyake et al., 2006]. A total of six copy number changes (four deletions and two duplications) were detected. One of them is copy number variations (CNVs) and four were unrelated to any genes. One 87-Kb duplication at 2q22.1 including *THSD7B* gene was found, but was maternally inherited based on the qPCR checking. No copy number change was found in *PLP1* or *DDR2* in these arrays.

DISCUSSION

This patient displayed two main symptoms simultaneously, that is, those of central neurological abnormalities and bone dysplasia. Regarding the central neurological symptoms, diffuse high intensity in the cerebral white matter in T2-weighed MRI images has not changed and is not progressive, and MBP and the oligoclonal band were negative in his CSF. In addition, inherited metabolic disorders resulting in demyelination, such as metachromatic leukodystrophy (MLD), globoid-cell leukodystrophy (GLD), and adrenoleukodystrophy (ALD), were excluded by enzymatic analysis or assay of very-long unsaturated fatty acids. MRS showing no increase in *N*-acetyl-asparatate (NAA) also indicated no demyelinating pattern. These lines of evidence indicate that neurological signs in this patient could be attributed to diffuse cerebral hypomyelination. Among the disorders presenting central dysmyelination, deletion 18q, Cockayne syndrome (#OMIM 216400), hypomyelination and atrophy of the basal ganglia and cerebellum (H-ABC) [van der Knaap et al., 2002], sialic acid storage disease (Salla disease; #OMIM 269920) and Tay syndrome (#OMIM 272800) were excluded by clinical history and physical examination. His neurological symptoms and findings of ABR and MRI are reminiscent of Pelizaeus–Merzbacher Disease (PMD) or Pelizaeus–Merzbacher-like Disease (PMLD; #311601). In our case, delay of the motor development appeared around 1 year of age, and his clinical symptoms slowly progressed thereafter. Furthermore, neurological signs including nystagmus, psychomotor deterioration, dysarthria, and optic atrophy and MR finding of preserved myelination in the internal capsule were compatible with the findings of the classical PMD. However, neither duplication nor mutation in the *PLP1* gene was detected.

Previous reports on spondylo-epi-metaphyseal dysplasia with short limb-abnormal calcification (hand) type suggest the possibility of autosomal recessive inheritance [al-Gazali et al., 1996; Cormier-Daire, 2008]; however, our case shows no mutation on *DDR2* gene.

There is one report describing a case with hypomyelinating leukoencephalopathy and metaphyseal chondrodysplasia, which maps to Xq25–27 [Neubauer et al., 2006]. The clinical course and brain MRI of that case is similar to those of our case, which are compatible with classical PMD. However, our patient had no deletion on chromosome level in the area Xq25–27. Furthermore, the pattern of skeletal abnormality is different from our case, in which the distal ulna, radius, distal femur, and proximal tibia showed significant involvement whereas the vertebrae and pelvis remained almost entirely unaffected (Table I).

Regarding the coexistence of skeletal abnormalities and neurological symptoms, Schimke immune-osseous dysplasia (SIOD) and spondyloenchondrodysplasia with spasticity, cerebral calcifications and immune dysregulation (SPENCD) should also be differentiated. The former does not have metaphyseal dysplasia and hypomyelination similar to our case is not reported previously in SIOD [Deguchi et al., 2008]. The latter is characterized by the specific radiographic features. Our patient did not show enchondroma on X-ray, cerebral calcification in CT and immune dysregulation [Renella et al., 2006]. Dyggve–Melchior–Clausen syndrome and Spondylo-epimetaphyseal dysplasia: a new X-linked variant with

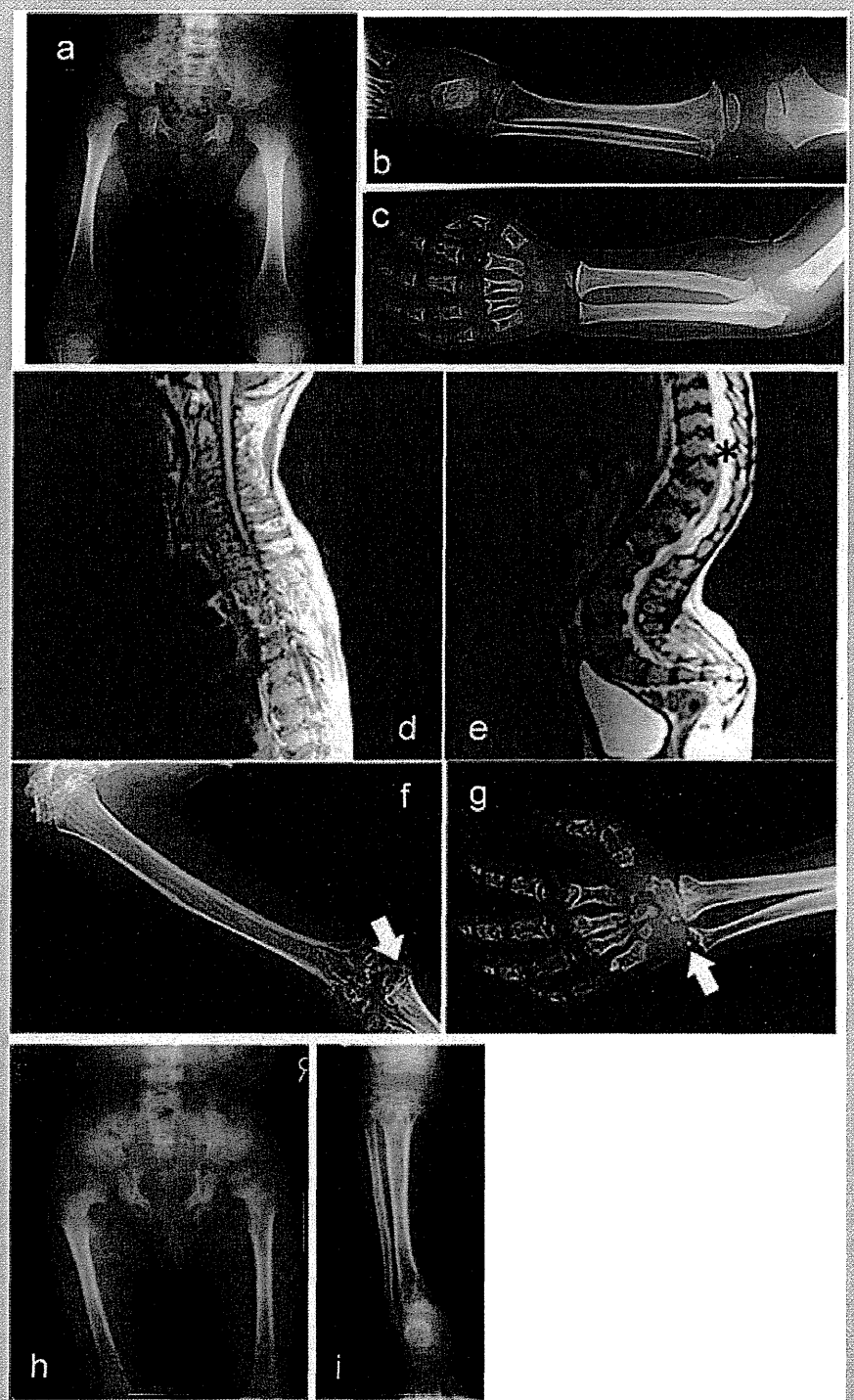

FIG. 2. Four years of age (a–c): (a) In the pelvis, upper acetabular margins are convexed and femoral heads are flattened. b: Metaphyses of Proximal tibia and distal femur are wide and flattened. The deformity of metaphyses is severer in upper limbs than lower ones. c: Proximal radius and ulnae are flared and broad. The appearances of epiphyses are delayed. 11 years of age (d–i): In the thoracic (d) and lumbar (e) spine, MRI of the spine shows flat and deformed vertebrae with wide and irregular intervertebral spaces. Lordosis is present. The spinal canal has enough space, and there is no spinal cord compression. f: The humerus is curved and shows radiolucency; and the distal end of metaphysis is broad and flared. Ossification of the epiphysis of the humerus is delayed for the age of 11 years and that of the ulna is absent (arrow). In (g), the metaphyses of both the radius and ulna are broad and flared at their distal ends. Stippled calcification is present in the distal end of the ulna. The epiphysis of the radius is present with soft tissue calcification around it. Small carpal bones are retarded in growth for the age of the patient. Metacarpal bones are short, the distal ends of metaphyses are broad, and the epiphyses are retarded for his age. The phalanges are short with corn-shaped epiphyses. h: In the pelvis, upper acetabular margins are convexed and femoral heads are flattened. The Ischia is short. i: Lower limbs. The distal femoral and proximal tibial metaphysis are wide and flattened. Stippled calcification is present on the epiphysis of proximal tibial bone.